Tully Fisher Relation for Disk Galaxies

Varenya Upadhyaya - EP20BTECH11026

Supervisor: Prof. Shantanu Desai

IITH

Outline

Abstract

Abstract

Objective

- The Tully Fisher relation is tight correlation between the luminosity of a galaxy and the width of its global HI profile
- The luminosity serves as a proxy to the stellar mass of the galaxy, while the HI line-width is an indicator of the circular velocity.
- The relation has been widely used to determine galaxy distances, estimate the value of the Hubble constant, and study local galaxy flows.
- In this project we study the relation at two different redshifts ($z \sim 0$ and $z \sim 1$)

Introduction

Introduction

Tully-Fisher Relation

- The Tully Fisher relation is tight correlation between the luminosity of a galaxy and the width of its global HI profile
- The luminosity serves as a proxy to the stellar mass of the galaxy, while the HI line-width is an indicator of the circular velocity.
- The relation has been widely used to determine galaxy distances, estimate the value of the Hubble constant (which was proposed to be 84km/s/Mpc in the original 1977 paper), and study local galaxy flows.

Introduction

The 1977 Paper

- Relation between the Absolute Magnitude (or luminosity) and the global HI line width

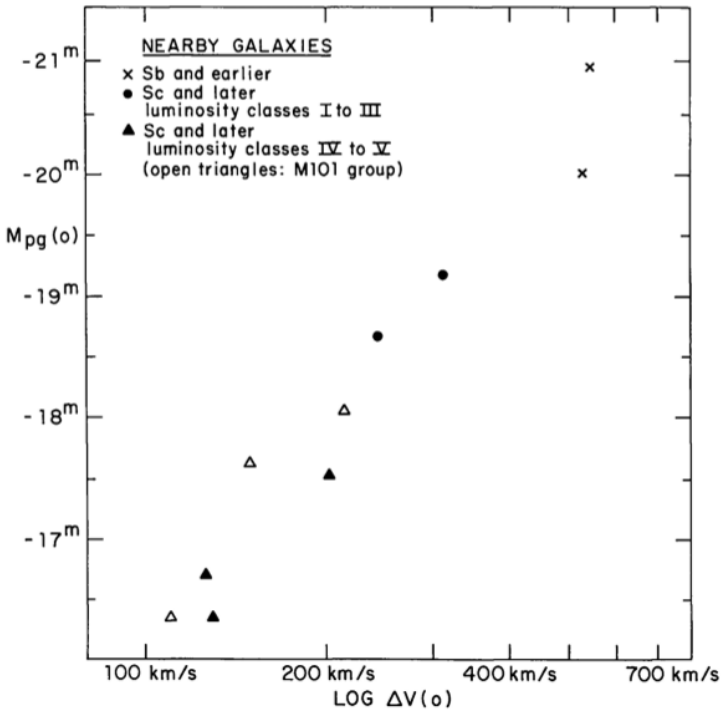

Fig. 1. Absolute magnitude – global profile width relation for nearby galaxies with previously well-determined distances. Crosses are M31 and M81, dots are M33 and NGC 2403, filled triangles are smaller systems in the M81 group and open triangles are smaller systems in the M101 group

The 1977 Paper

- Relation between the Absolute Magnitude (or luminosity) and the global HI line width

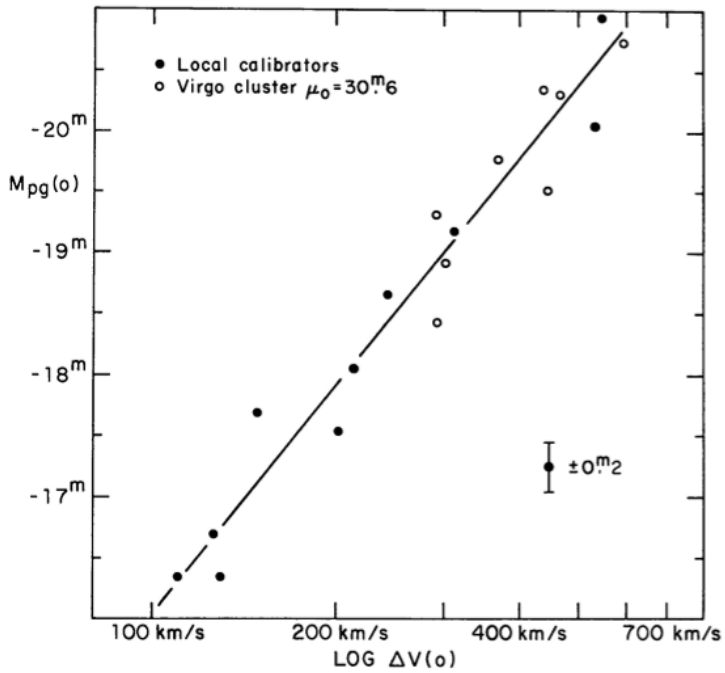

Fig. 5 (a) Absolute magnitude – global profile width relation produced by overlaying Figure 3 on Figure 1, adjusting Figure 3 vertically to arrive at a best visual fit with a distance modulus of $\mu_0 = 30^m.6 \pm 0^m.2$

Introduction

Tully-Fisher Relation

- A more fundamental relation than the standard TFR appears when we use baryonic mass and circular velocity
- This new relation is known as the Baryonic TFR

$$M_{bar} = M_{star} + M_{gas} \tag{1}$$

$$M_{bar} = \frac{(V_f)^{\alpha}}{\beta} \tag{2}$$

In the log scale:

$$\log M_{bar} = m \log V_f + b \tag{3}$$

Similarly the "Stellar" TFR is written as:

$$\log M_{star} = m \log V_f + b \tag{4}$$

Introduction

The physics behind the TFR is still disputed

- $\alpha = 4$ is currently the accepted value for the slope
- ΛCDM suggests $\alpha = 3$ and $\beta = 10 f_v^3 G H_0$ where f_v relates the observed V_f to the V_c at the virial radius
- MOND (Modified Newtonian Dynamics) predicts an acceleration relation $a_0 = V_f^4 / GM$ which is consistent with the slope
- The BTFR is also related to Radial Acceleration Relation (an empirical scaling law between the total and baryonic accelerations in galaxies)
- A discussion on the occurrence of the TFR is beyond the scope of this presentation.

Introduction

Markov-Chain Monte Carlo Sampling `emcee`

- Broadly speaking, MCMC methods are used to numerically perform multidimensional integrals
- For our purposes, they're used to find the "most likely" parameters that model some data.
- In essence, the whole process consists of comparing a model (generated using some parameters) against some data and sampling the parameters that best fit the data
- MCMC simulations are inherently Bayesian methods, as they require some *prior* knowledge of the parameters

Data

Data

Z∼0

- We use the SPARC (Spitzer Photometry & Accurate Rotation Curves) database which is a sample of 175 nearby galaxies
- The data can be found at SPARC Homepage
- For our analysis, we use the table provided under the Baryonic Tully Fisher Relation section.
- While the masses are a sorted out affair, the right definition for circular velocity is a little ambiguous, there are 6 definitions to consider

Data

Z∼0: velocity definitions

1. W_{P20} is the line-width measured at 20% of the peak flux density of the global H I profile (this definition was used in the original paper).
2. W_{M50} is the line-width measured at 50% of the mean flux density of the global H I profile. $W_{M50}<W_{P20}$, implying that W_{M50} probes velocities at smaller radii.
3. V_{max} is the circular velocity measured at the peak of the observed rotation curve, usually $V_{max}>V_{2.2}$
4. V_{2R_e} is the circular velocity measured at $2R_e$ where R_e is the effective radius encompassing half of the galaxy luminosity.
5. $V_{2.2}$ is the circular velocity measured at $2.2R_d$ (R_d is the disc scale length)
6. V_f is the average circular velocity along the flat part of the rotation curve.

Data

z∼1

- For higher redshifts, we used the KROSS data
- The KMOS Redshift One Spectroscopic Survey (KROSS)is an ESO-guaranteed time survey of 795 typical star-forming galaxies in the redshift range $z = 0.8$-1.0 with the KMOS instrument on the Very Large Telescope.
- Out of these, [2] analysed 344 galaxies out which we use 250 galaxies for our purposes.
- The analysed data investigated the circular velocity at three length scales:

Data

z∼1 length scales

1. R_e (Effective radius)
2. $R_{opt} = 3.2R_D$ (Optical radius)
3. $R_{out} = 6.4R_D$ (Twice the optical radius)
4. R_D=0.59R_e is the disk length

Since the effective radius for the majority of samples falls below resolution limit and the optical radius stays on the verge, our analysis is restricted to the measurements done at R_{out}

Analysis

Analysis

emcee specifications

- Eqs. 3 and 4 represent our parametric model
- Uniform priors for $m, b \in [-10, 10]$ and $\sigma_{int} \in [-1, 1]$
- We use three separate likelihoods for our analysis

Likelihoods

1. A χ^2 likelihood that follows:

$$-2\mathcal{L} = \sum \left(\frac{y_i - (mx_i + b)}{\sigma_y} \right)^2, \tag{5}$$

Analysis

Likelihoods

2. A simple log-likelihood ($\mathcal{L}_1$ from here on)

$$-2ln\mathcal{L}_1 = \sum_i (2\pi\sigma_i^2) + \sum_i \frac{(y_i - mx_i - c)^2}{\sigma_i^2} \tag{6}$$

$$\sigma_i^2 = m^2\sigma_{x_i}^2 + \sigma_{y_i}^2 + \sigma_{int}^2 \tag{7}$$

3. A slightly more complicated routine ($\mathcal{L}_2$ from here on)

$$-2ln\mathcal{L}_2 = \sum_i (2\pi\sigma_i^2) + \sum_i \frac{(y_i - mx_i - c)^2}{\sigma_i^2(m^2+1)} \tag{8}$$

$$\sigma_i^2 = \frac{m^2\sigma_{x_i}^2 + \sigma_{y_i}^2}{m^2+1} + \sigma_{int}^2 \tag{9}$$

where σ_i represents the intrinsic scatter (a measure of how much the model deviates from the data).

Results

Params for $z \sim 0$

Velocity	Slope	Intercept	Intrinsic Scatter	Number of galaxies
V_f	$3.63^{+0.08}_{-0.09}$	$2.45^{+0.18}_{-0.18}$	$0.11^{+0.02}_{-0.03}$	123
$W_{P20}/2$	$3.53^{+0.07}_{-0.07}$	$1.37^{+0.18}_{-0.18}$	$0.13^{+0.02}_{-0.02}$	148
$W_{M50}/2$	$3.40^{+0.09}_{-0.09}$	$1.79^{+0.21}_{-0.21}$	$0.13^{+0.02}_{-0.02}$	125
V_{max}	$3.31^{+0.07}_{-0.07}$	$3.04^{+0.15}_{-0.15}$	$0.15^{+0.02}_{-0.02}$	153
V_{2R_e}	$2.92^{+0.07}_{-0.07}$	$4.00^{+0.15}_{-0.15}$	$0.17^{+0.02}_{-0.02}$	142
$V_{2.2}$	$2.81^{+0.07}_{-0.07}$	$4.27^{+0.15}_{-0.15}$	$0.21^{+0.02}_{-0.02}$	148

Table: The best fit parameters for different velocity definitions in the SPARC data using $\mathcal{L}_1$

Figures for $z \sim 0$

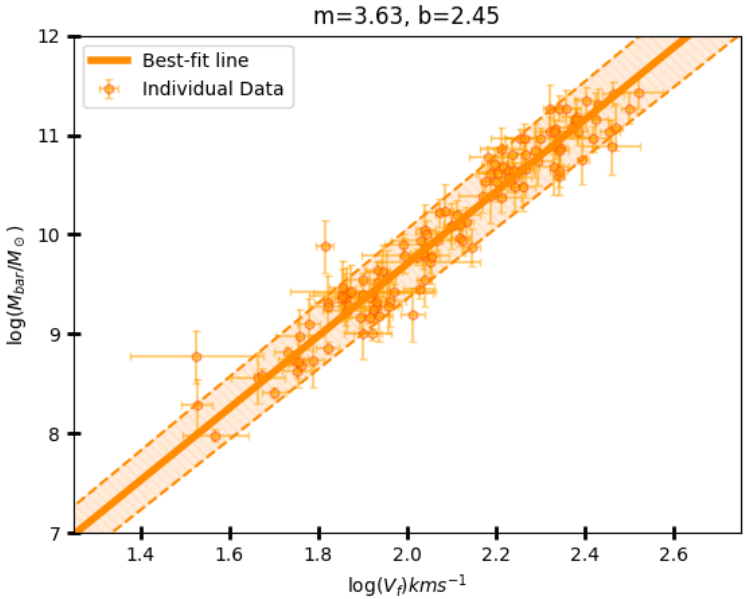

(a) A plot of the data points (along with the errorbars) over the model.

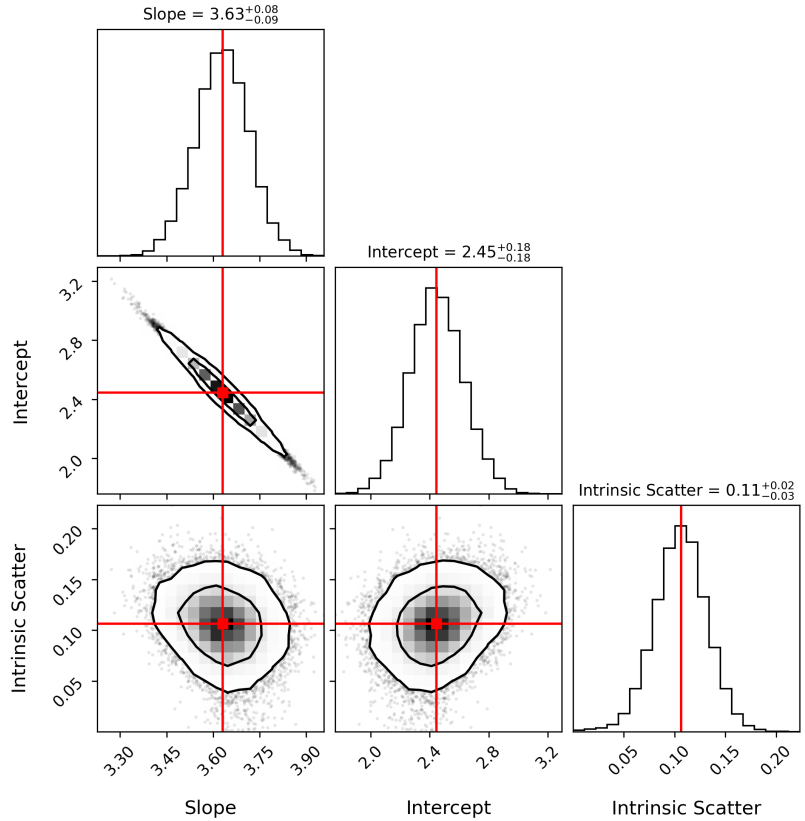

(b) The cornerplot for V_f which depicts the posterior distributions for the parameters.

Figure: The best fit and corner plot for V_f using our likelihood.

Bestfit plots for $z \sim 0$

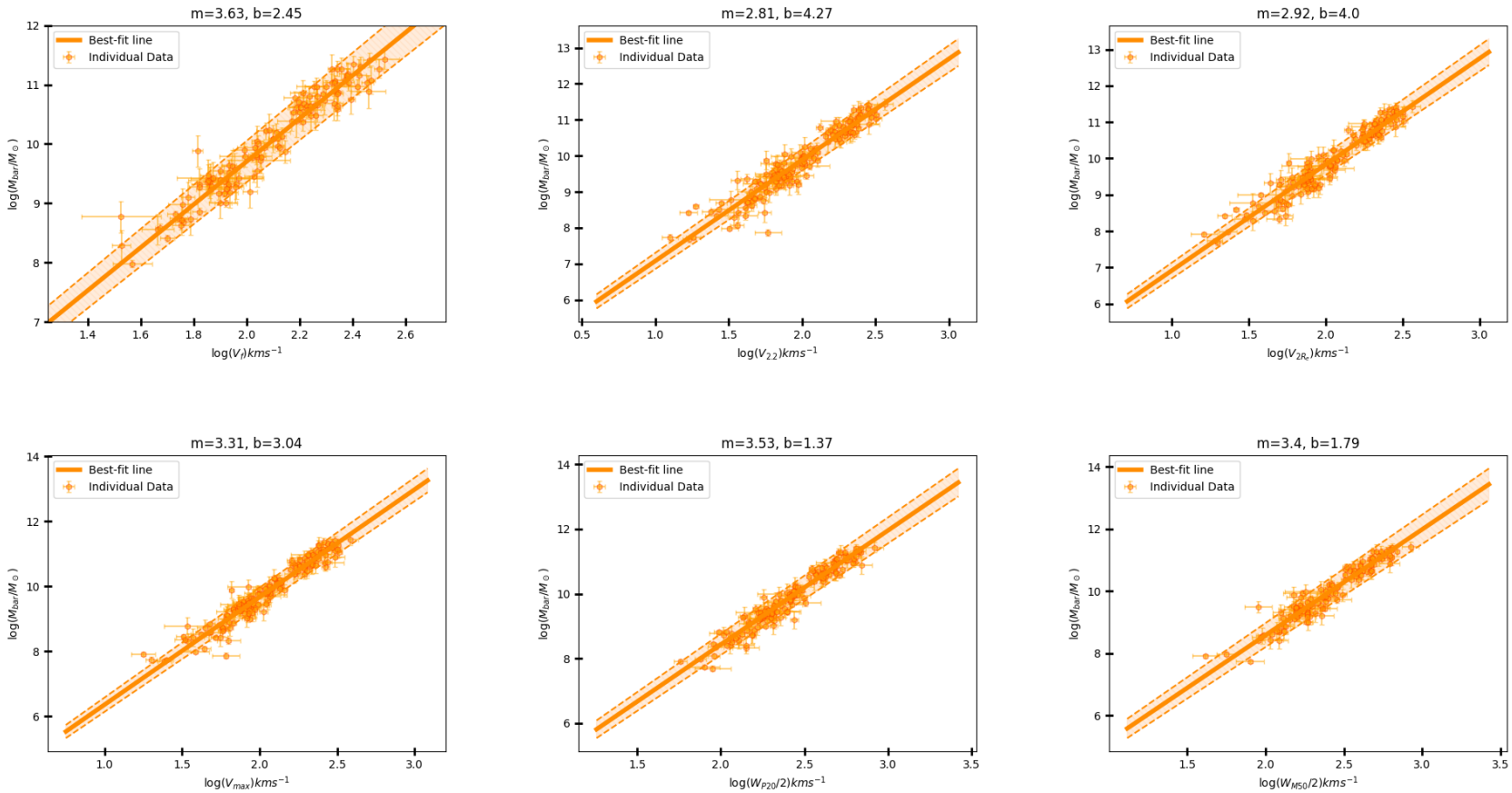

Figure: The BTFR for different velocity definitions:V_f(top left), $V_{2.2}$(top middle), V_{2R_e}(top right),V_{max} (bottomleft),$W_{P20}/2$(bottom middle),and $W_{M50}/2$(bottom right).The black line shows a linear fit to the data.The tightest and steepest BTFR is given by V_f

Results for $z \sim 1$

For galaxies in the one redshift range, we first ran our code for masses that were calculated using certain scaling relations that are powerful enough to give the total masses of the systems. Since circular velocities are only computed up to the visible domain, we later scaled these masses down using a Sersic Profile:

$$M_{gas}(R) = M_{gas}\left\{1 - \left(1 + \frac{R}{R_D}\right) e^{-R/R_D}\right\} \tag{10}$$

$$M_{star}(R) = M_{star}\left\{1 - \left(1 + \frac{R}{R_D}\right) e^{-R/R_D}\right\} \tag{11}$$

Params (at full mass)

Likelihood	Mass	m	b	σ_{int}
χ^2	Baryonic	$-0.09^{+0.14}_{-0.14}$	$11.28^{+0.30}_{-0.31}$	–
χ^2	Stellar	$+0.86^{+0.07}_{-0.07}$	$8.14^{+0.16}_{-0.16}$	–
$\mathcal{L}_1$	Baryonic	$-0.09^{+0.14}_{-0.14}$	$11.26^{+0.30}_{-0.30}$	$0.00^{+0.06}_{-0.06}$
$\mathcal{L}_1$	Stellar	$+0.91^{+0.13}_{-0.13}$	$8.04^{+0.28}_{-0.29}$	$0.26^{+0.02}_{-0.02}$
$\mathcal{L}_2$	Baryonic	$-0.02^{+0.03}_{-0.03}$	$10.96^{+0.70}_{-0.70}$	$0.14^{+0.01}_{-0.01}$
$\mathcal{L}_2$	Stellar	$+3.95^{+0.73}_{-0.57}$	$1.38^{+1.26}_{-1.59}$	$0.00^{+0.02}_{-0.02}$

Table: The best fit parameters for the KROSS data before scaling the masses

BTFR for $z \sim 1$ before scaling the masses down

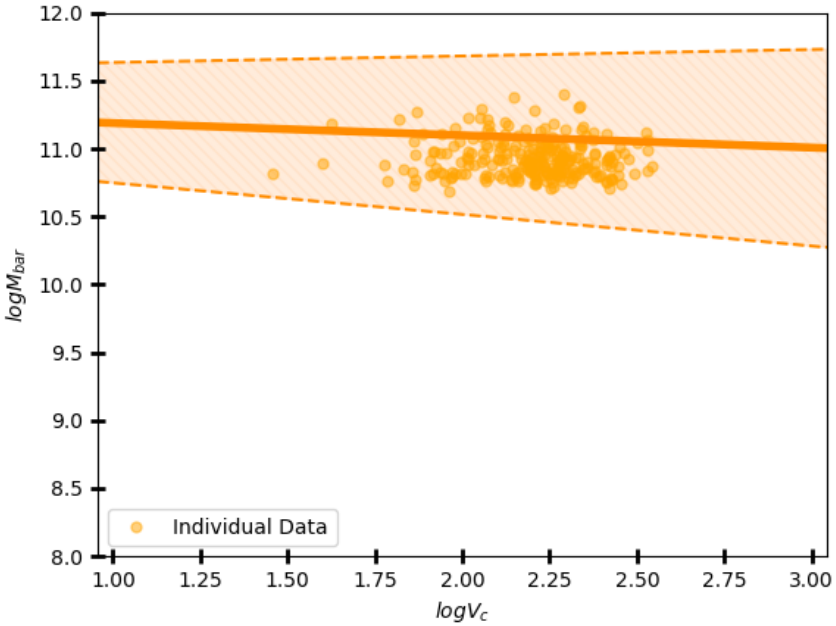

(a) Best Fit - χ^2

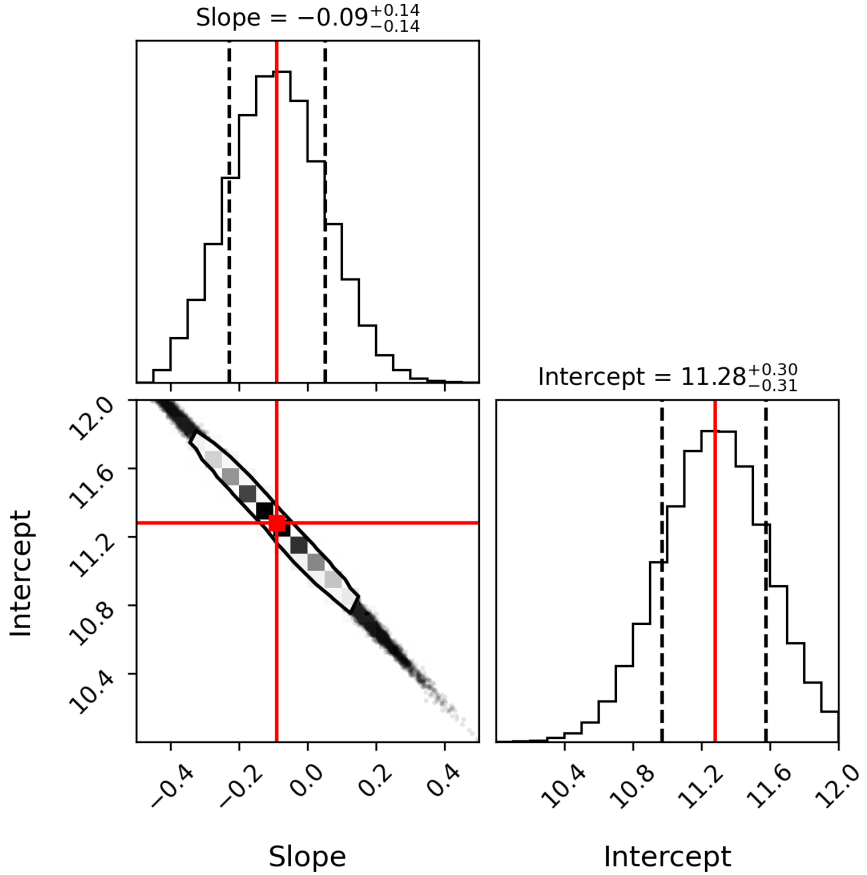

(b) Cornerplot - χ^2

BTFR for $z \sim 1$ before scaling the masses down

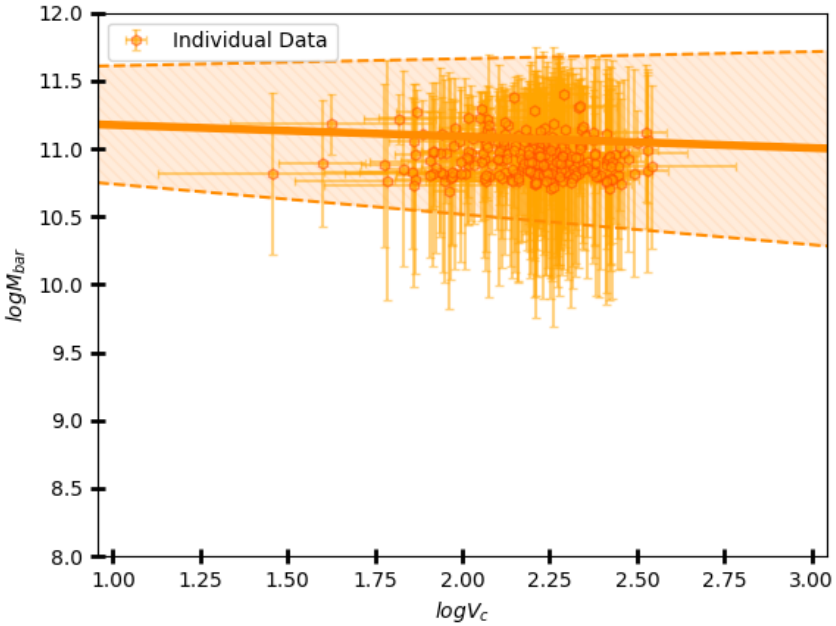

(a) Best Fit - $\mathcal{L}_1$

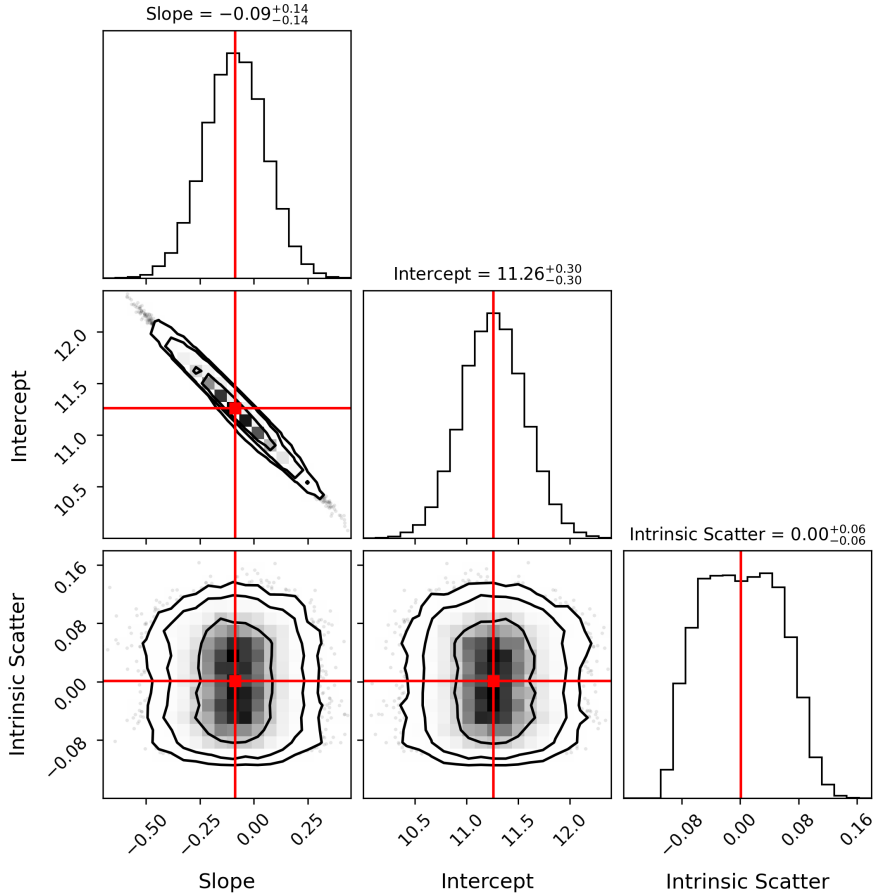

(b) Cornerplot - $\mathcal{L}_1$

BTFR for $z \sim 1$ before scaling the masses down

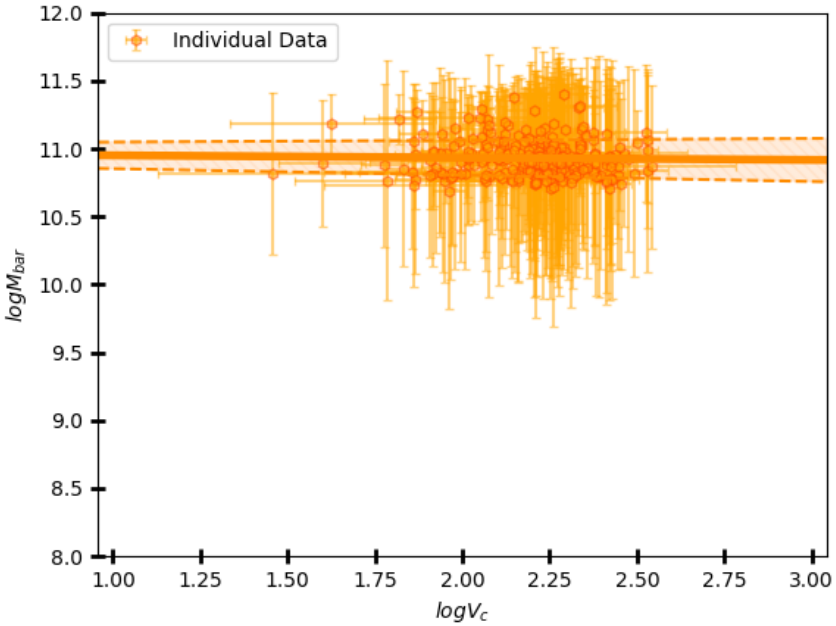

(a) Best Fit - $\mathcal{L}_2$

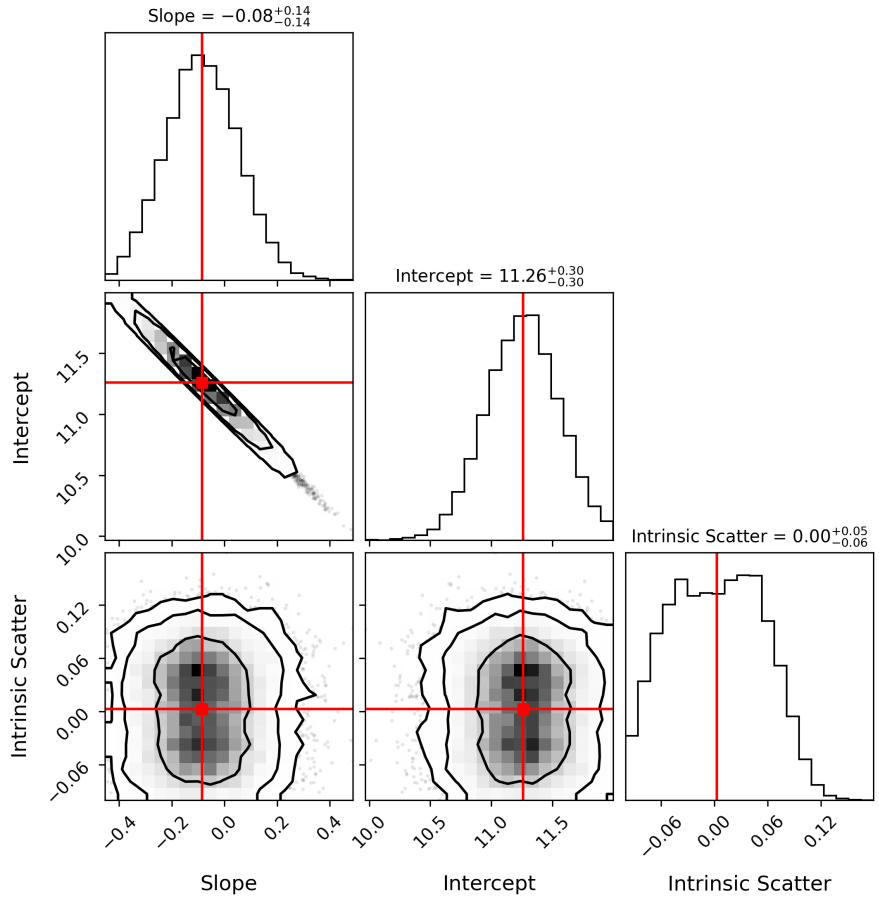

(b) Cornerplot - $\mathcal{L}_2$

STFR for $z \sim 1$ before scaling the masses down

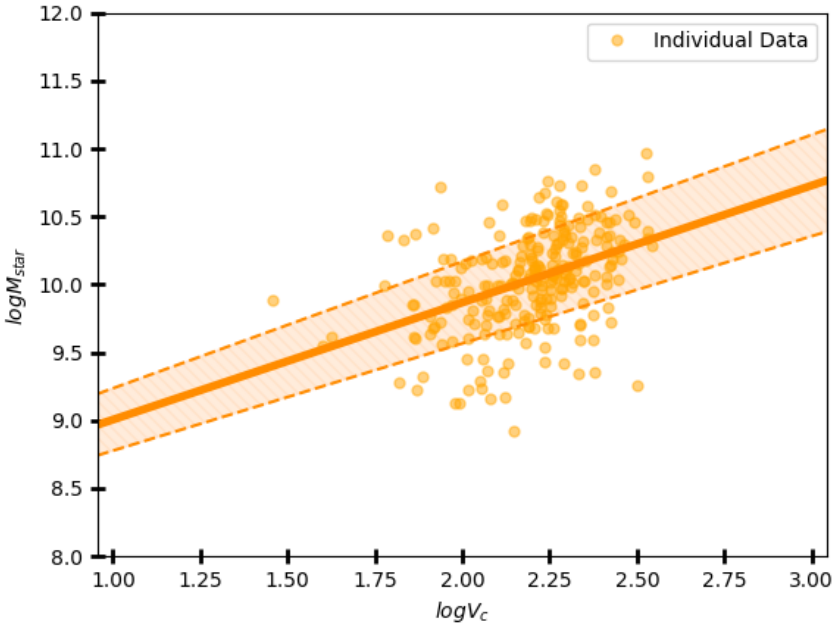

(a) Best Fit - χ^2

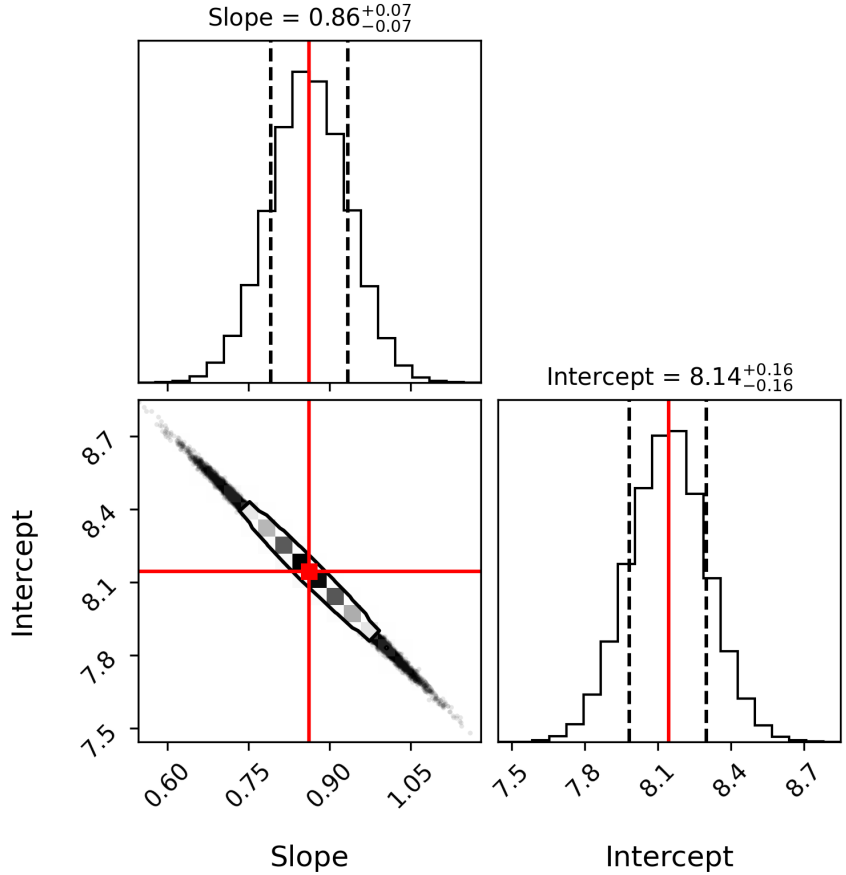

(b) Cornerplot - χ^2

STFR for $z \sim 1$ before scaling the masses down

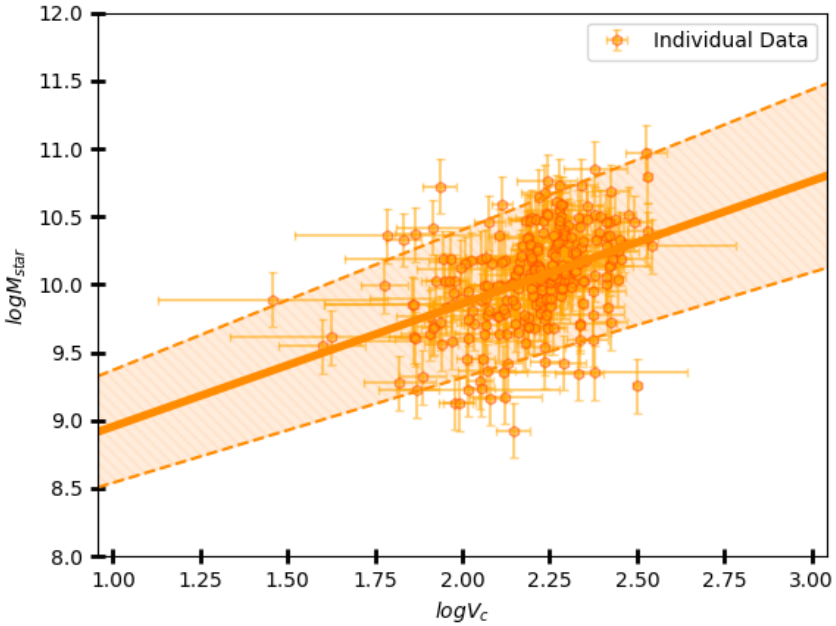

(a) Best Fit - $\mathcal{L}_1$

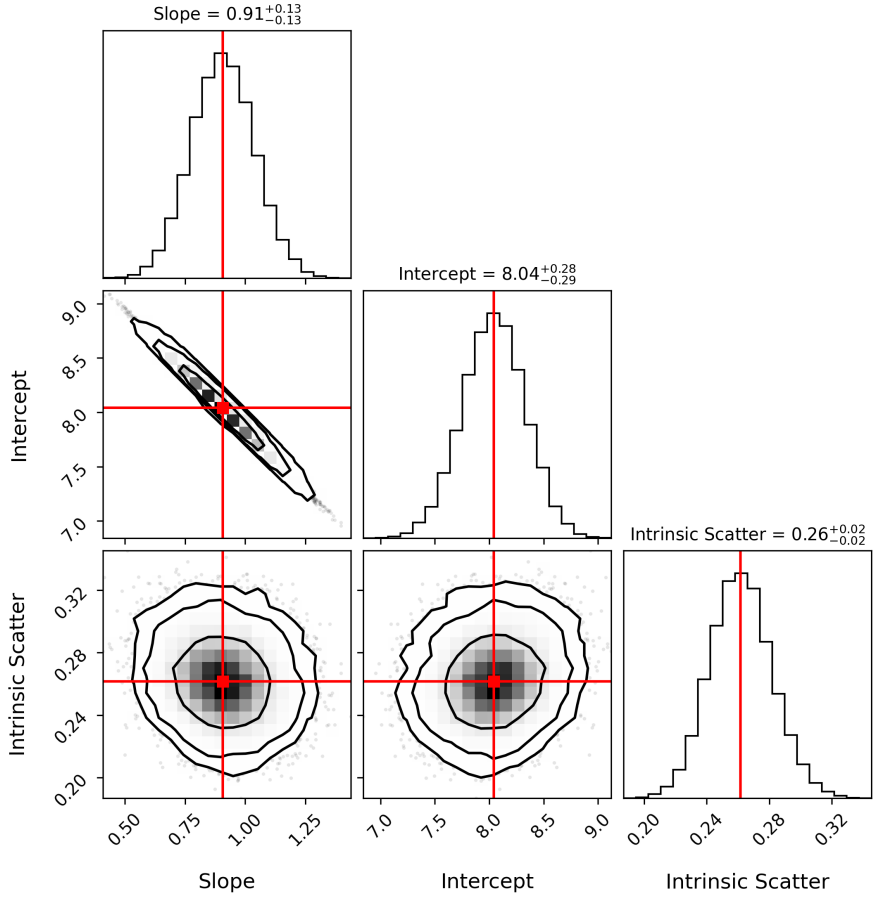

(b) Cornerplot - $\mathcal{L}_1$

STFR for $z \sim 1$ before scaling the masses down

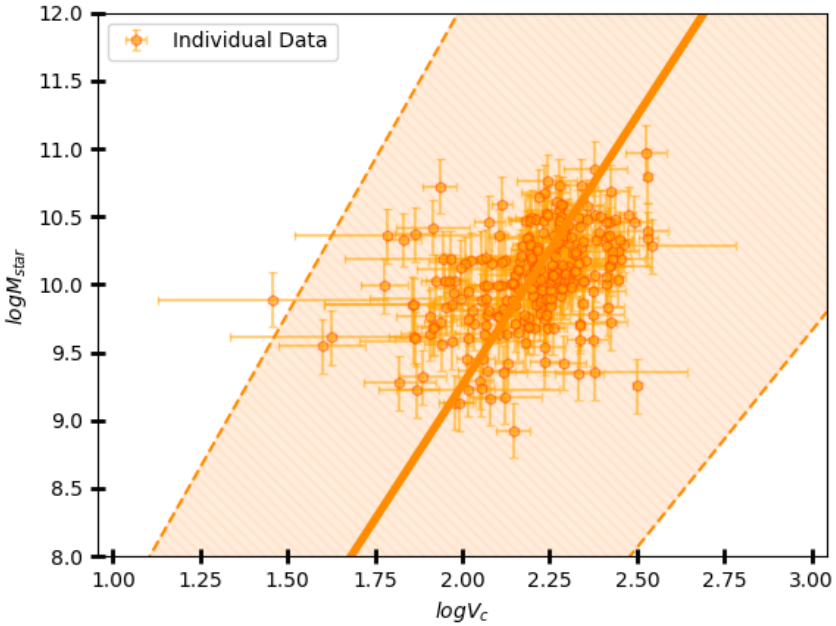

(a) Best Fit - $\mathcal{L}_2$

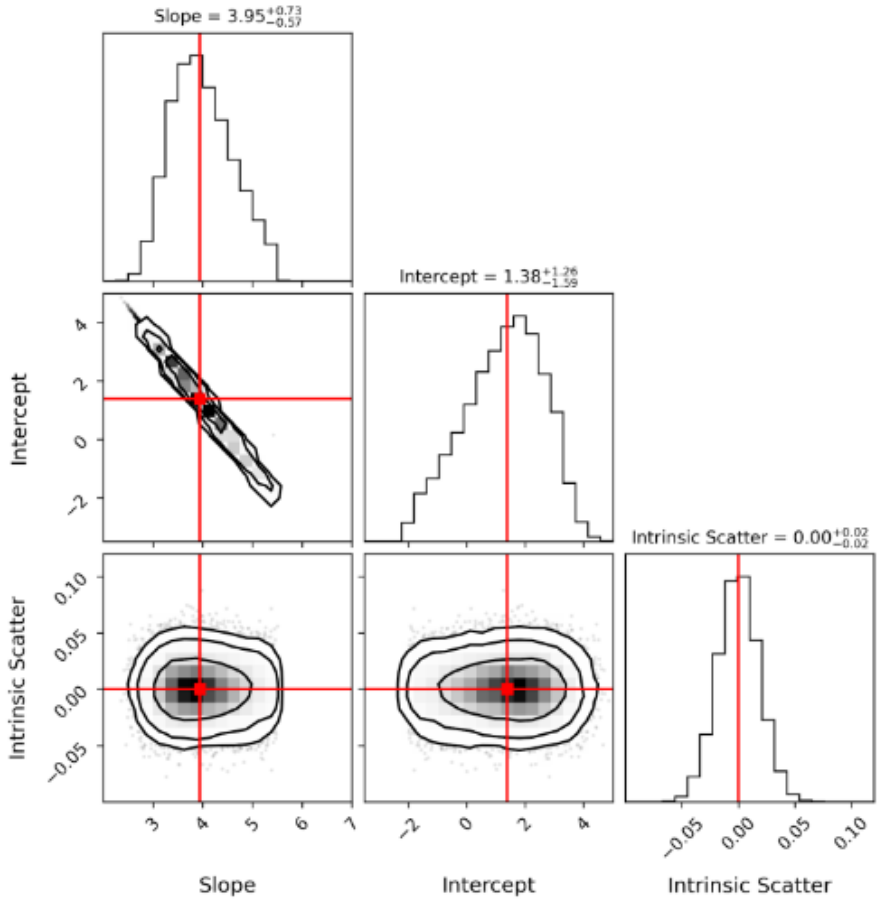

(b) Cornerplot - $\mathcal{L}_2$

Params for $z \sim 1$ after scaling the masses down

Likelihood	Mass	m	b	σ_{int}
χ^2	Baryonic	$0.16^{+0.11}_{-0.11}$	$10.18^{+0.24}_{-0.24}$	8.16
χ^2	Stellar	$0.90^{+0.08}_{-0.08}$	$8.02^{+0.18}_{-0.18}$	29.94
$\mathcal{L}_1$	Baryonic	$0.17^{+0.13}_{-0.12}$	$10.13^{+0.28}_{-0.28}$	$0.09^{+0.02}_{-0.03}$
$\mathcal{L}_1$	Stellar	$1.03^{+0.15}_{-0.15}$	$7.75^{+0.32}_{-0.33}$	$0.26^{+0.02}_{-0.02}$
$\mathcal{L}_2$	Baryonic	$0.80^{+0.16}_{-0.14}$	$8.70^{+0.30}_{-0.35}$	$0.11^{+0.03}_{-0.03}$
$\mathcal{L}_2$	Stellar	$4.02^{+0.74}_{-0.62}$	$1.11^{+1.36}_{-1.59}$	$0.00^{+0.02}_{-0.02}$

Table: The best fit parameters for the KROSS data after scaling the masses

BTFR for $z \sim 1$ after scaling the masses down

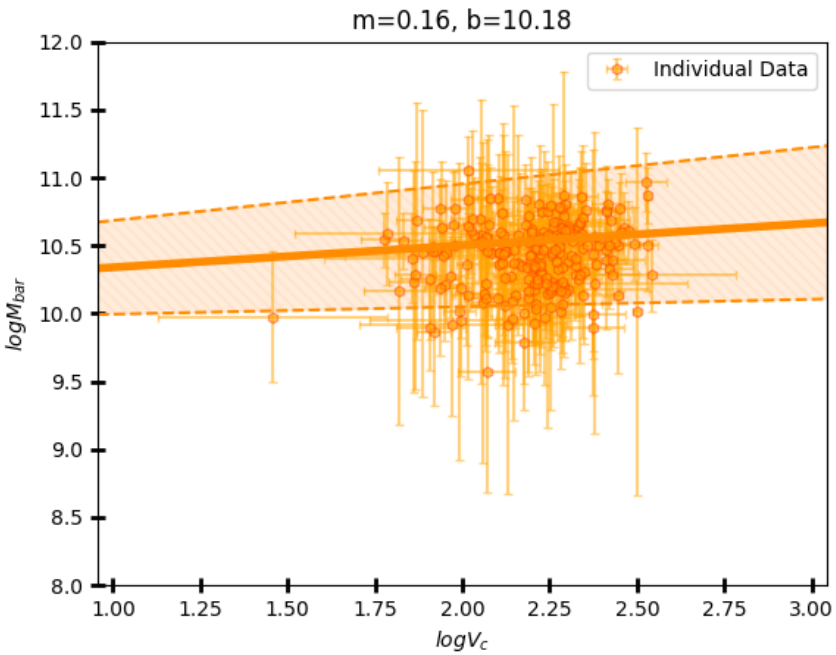

(a) Best Fit - χ^2

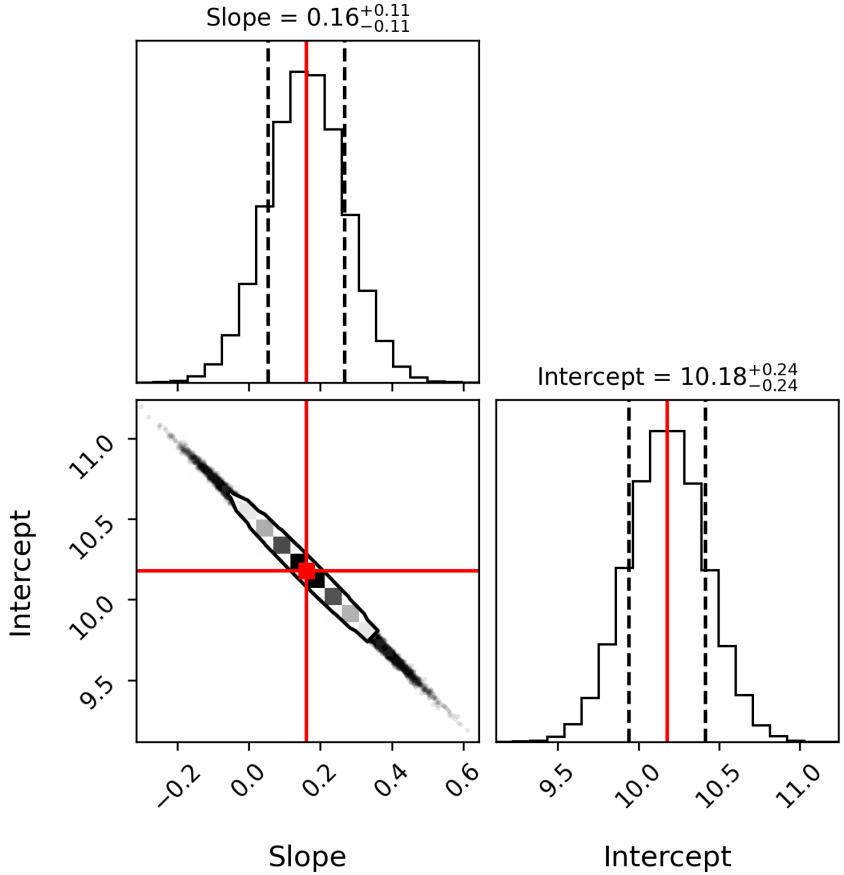

(b) Cornerplot - χ^2

BTFR for $z \sim 1$ after scaling the masses down

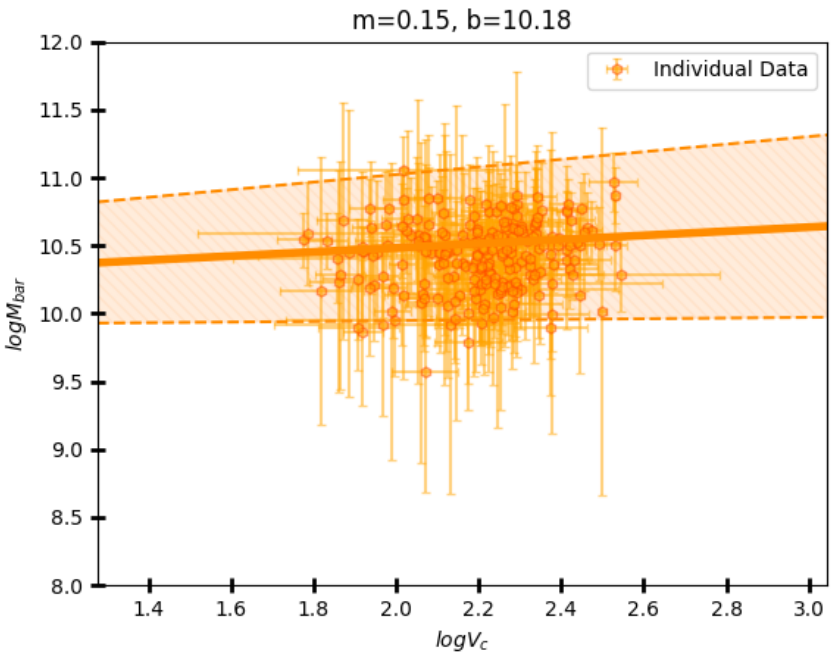

(a) Best Fit - $\mathcal{L}_1$

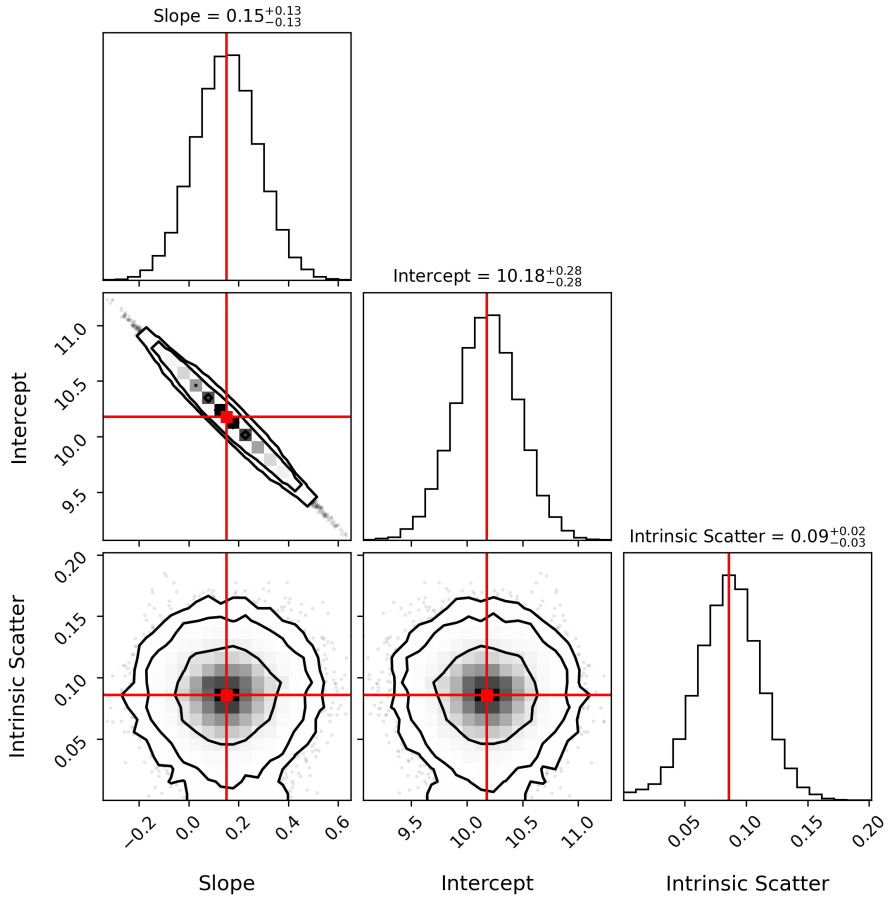

(b) Cornerplot - $\mathcal{L}_1$

BTFR for $z \sim 1$ after scaling the masses down

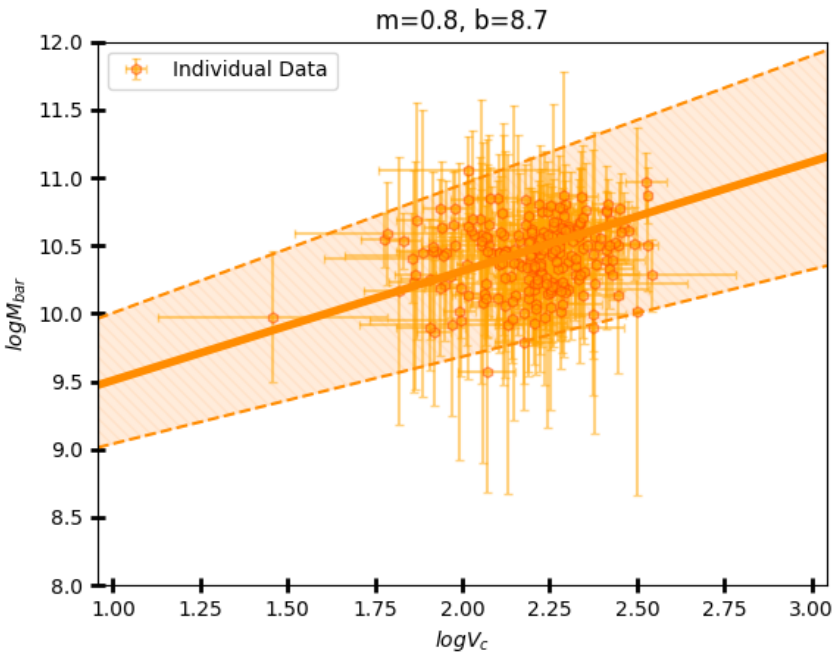

(a) Best Fit - $\mathcal{L}_2$

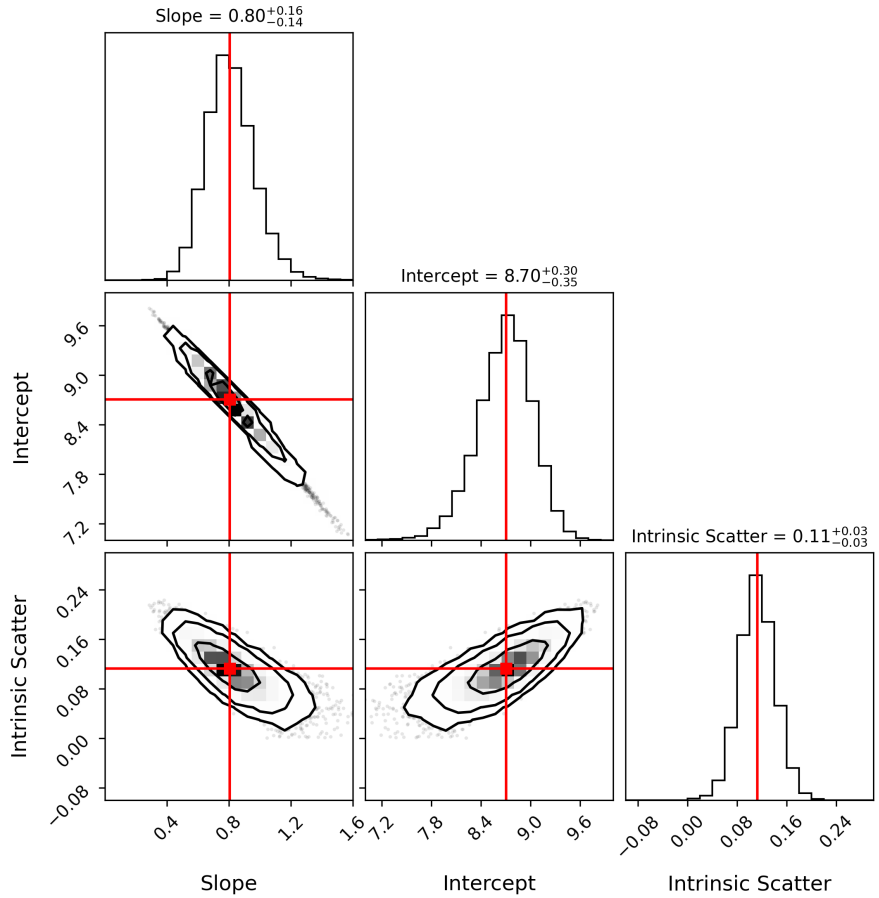

(b) Cornerplot - $\mathcal{L}_2$

STFR for $z \sim 1$ after scaling the masses down

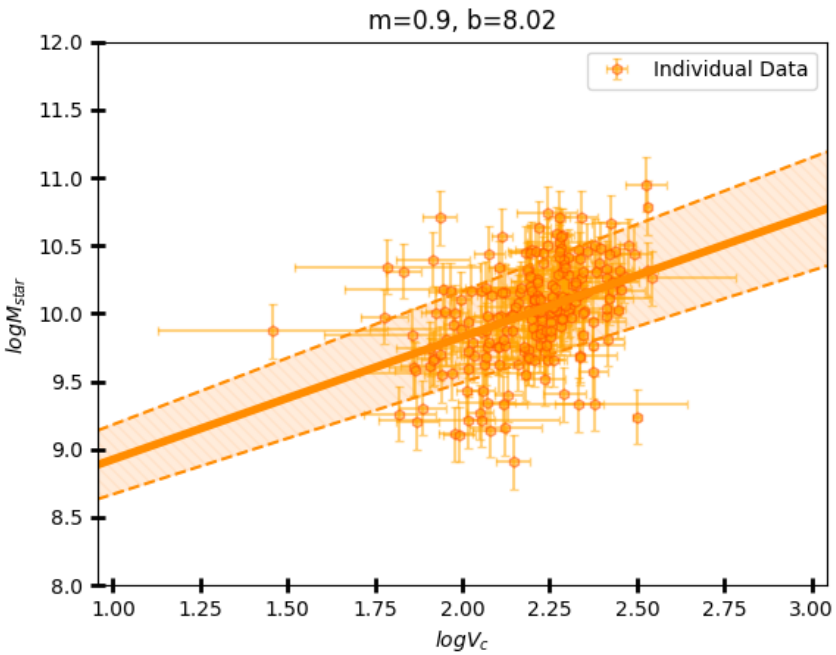

(a) Best Fit - χ^2

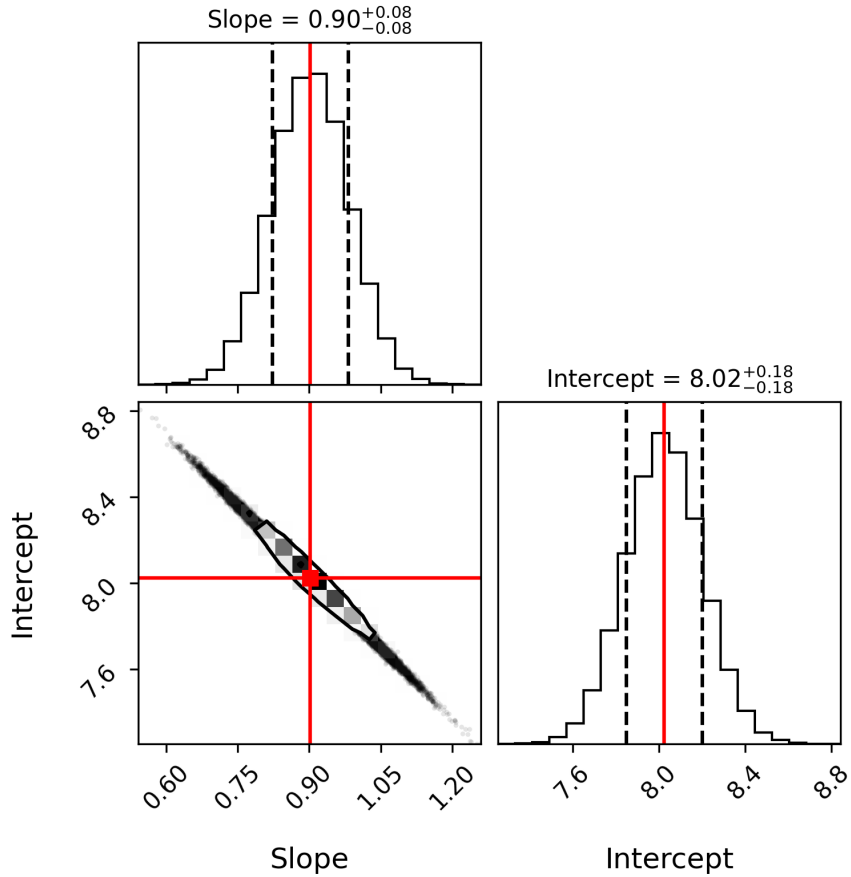

(b) Cornerplot - χ^2

STFR for $z \sim 1$ after scaling the masses down

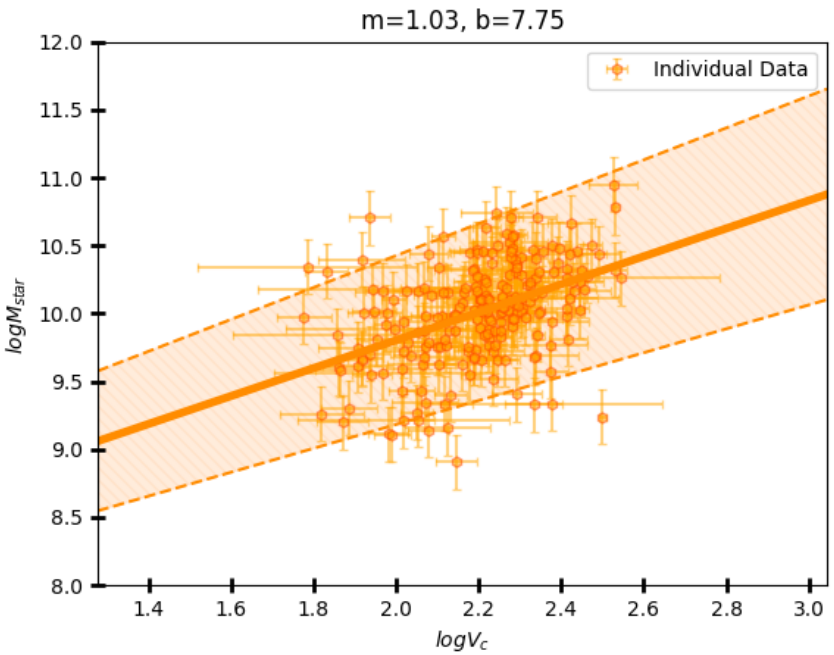

(a) Best Fit - $\mathcal{L}_1$

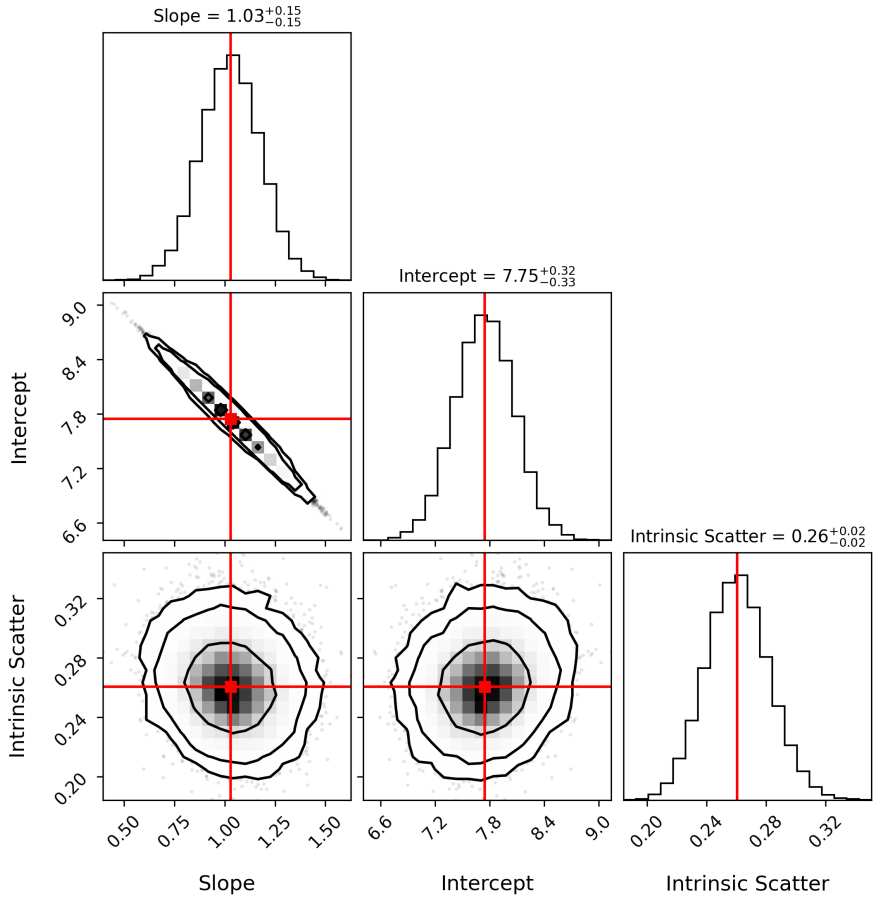

(b) Cornerplot - $\mathcal{L}_1$

STFR for $z \sim 1$ after scaling the masses down

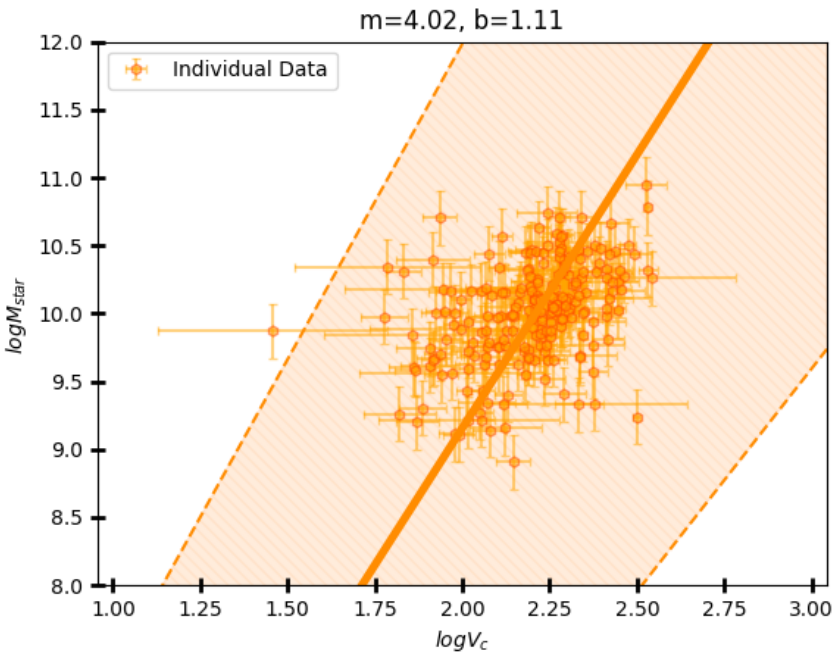

(a) Best Fit - $\mathcal{L}_2$

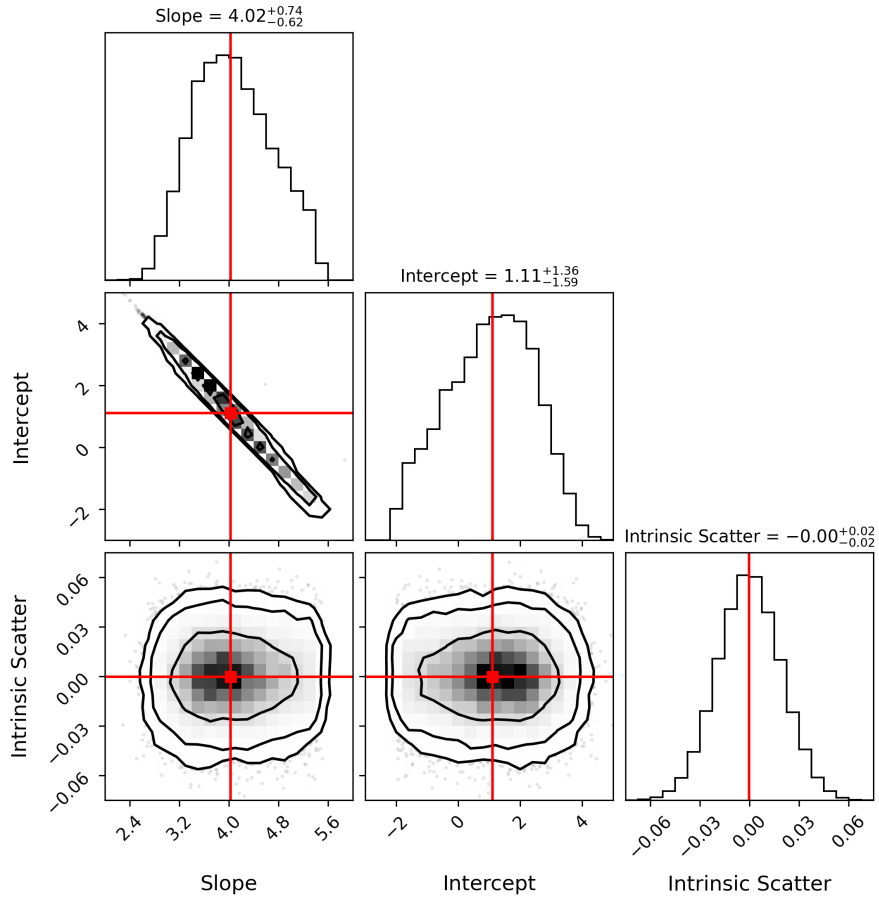

(b) Cornerplot - $\mathcal{L}_2$

Conclusions

Conclusions

Conclusions

- The slope and intercept parameters we attained for $z \sim 0$ agree with the ones in [1], meaning that we successfully recreated the results they did. We find that V_f shows the steepest slope and the least intrinsic scatter, making it a better velocity definition than the other 5 we considered.
- The slopes in $z \sim 1$ are very small for BTFR and $m \sim 1$ for STFR. This implies little-to-no correlation which could be due to the high errors in our data or due to the computations done to arrive at the values for the masses and velocities. This does not however, stand as the final conclusion to the project as we are still working on doing the analysis on bigger datasets at the same redshift.

Thank you!

Appendix

Appendix

Markov-Chain Monte Carlo Sampling

- Broadly speaking, MCMC methods are used to numerically perform multidimensional integrals
- For our purposes, they're used to find the "most likely" parameters that model some data.
- In essence, the whole process consists of comparing a model (generated using some parameters) against some data and sampling the parameters that best fit the data
- MCMC simulations are inherently Bayesian methods, as they require some *prior* knowledge of the parameters

Appendix

The probability of a model given a data is (using Bayes theorem):

$$P(\theta|D) = \frac{P(D|\theta) \times P(\theta)}{P(D)} \tag{12}$$

where $\theta \equiv$ Model and $D \equiv$ Data

- $P(\theta|D)$: Posterior Probability (probability of the model given the data)
- $P(D|\theta)$: Likelihood (probability of the data given the model)
- $P(\theta)$: Prior (the probability of the model)
- $P(D)$: Evidence (probability of the data, usually taken as unity)

Appendix

Using MCMC, we can estimate the posterior distribution by numerically integrating the RHS of (12). For the expectation value of θ, we would need:

$$E(\theta) = \int \theta p(\theta)\, d\theta \tag{13}$$

This integral is numerically calculated using the MCMC sampler

$$E(\theta) \approx \frac{1}{N} \sum_{n=1}^{N} \theta_n \tag{14}$$

Appendix

The Procedure

- Establish a function that outputs the model (in our case, a straight line)
- Initialize an ensemble of "walkers" defined by θ, a vector of parameters that contains the parameters in question. For example, a simple linear fit will have a θ like:

$$\theta = \begin{pmatrix} m \\ b \end{pmatrix}, \tag{15}$$

with m and b as the slope and intercept respectively

Appendix

The Procedure continued

- Every walker now begins to explore the parameter space (bounded by the prior) by taking "steps" (or walking) to new values of θ and comparing this model to the data using a *Likelihood Function*
- For a simple χ^2 likelihood (assuming a linear fit) this would look like:

$$-2\mathcal{L} = \sum \left(\frac{y_i - (mx_i + b)}{\sigma_y} \right)^2, \tag{16}$$

with σ_y representing the error in data.

- MCMC then checks the ratio of $\mathcal{L}$ generated by the new model v. the current model and moves to the new θ if it provides a better match.
- If this ratio is larger than a certain *acceptance ratio*, the θ moves to this new model

Appendix

The Procedure continued

- The acceptance ratio ensures that the model doesn't get stuck in individual peaks of high probabilities
- Eventually all the walkers end up "climbing" to the models with high $\mathcal{L}$ values
- After the code is done running, we're left with a *posterior distribution* with every walker keeping a record of every model it walked to.
- Assuming that the code ran for long enough to converge, we're left with a distribution that represents a sample of reasonable models for the data.

References

[1] Federico Lelli et al. "The baryonic Tully-Fisher relation for different velocity definitions and implications for galaxy angular momentum". In: 484.3 (Apr. 2019), pp. 3267–3278. DOI: 10.1093/mnras/stz205. arXiv: 1901.05966 [astro-ph.GA].

[2] Gauri Sharma et al. "Flat rotation curves of z $\sim$ 1 star-forming galaxies". In: *Monthly Notices of the Royal Astronomical Society* 503.2 (Feb. 2021), pp. 1753–1772. DOI: 10.1093/mnras/stab249. URL: https://doi.org/10.1093%2Fmnras%2Fstab249.